NASA Electric Aircraft Testbed (NEAT) Single-Aisle Transport Air Vehicle Hybrid Electric Tail-Cone Thruster Powertrain Configuration and Test Results

Rodger W. Dyson,[1]
NASA Glenn Research Center, Cleveland, OH, 44135, USA

A key technical challenge is to establish a viable concept for a MW-class hybrid gas-electric propulsion system for a commercial transport aircraft. This includes developing aircraft propulsion system conceptual designs, integrating sub-systems, high efficiency/power density electric machines, flight-weight power system and electronics, and enabling materials in high voltage insulation, high frequency soft magnetics, and conductors. The primary benefit of this research is to diversify the current turbofan propulsion options to include hybrid electric propulsion elements that reduce energy usage, emissions, and noise. A reconfigurable powertrain testbed at NASA Glenn Research Center is described including test results from the initial 500 kW powertrain configuration.

I. Nomenclature

COTS	=	Commercial off the Shelf
PLC	=	Programmable Logic Controller for facility management
DAQ	=	Data Acquisition System recording
STARC-ABL	=	Single-Aisle Turbo-electric Aircraft Aft Boundary Layer Ingestion
ARINC	=	Aeronautical Radio Incorporated
PowerDNA	=	Compact cube interfaces to Simulink and communications
GUI	=	Graphical User Interface
AC	=	Alternating Current
DC	=	Direct Current
CANbus	=	Controller Area Network bus
UDP	=	User Datagram Protocol
NPSS	=	Numerical Propulsion System Simulator
PLA	=	Power Lever Angle
FADEC	=	Full Authority Digital Engine Control
Wf	=	Gas Generator Fuel Flow
T-MATS	=	Toolbox for the Modeling and Analysis of Thermodynamic Systems

II. Introduction

NASA's Electric Aircraft Test bed (NEAT) is being developed to enable end-to-end development and testing of a full-scale electric aircraft powertrain. The primary purpose of the test bed is to enable the high-power ambient and cryogenic flight-weight power system testing that is required for the development of the following components to Technology Readiness Level (TRL) 6: (Dyson, 2016)

- **High-voltage bus architecture**—Insulation and geometry; 600 to 4500 V
- **High-power megawatt inverters and rectifiers**—Commercial, in-house, and NASA Research Announcement (NRA) development
- **High-power megawatt motors and generators**—Commercial, in-house, and NRA development

[1] Hybrid Gas Electric Propulsion Technical Lead, Thermal Energy Conversion Branch, and AIAA Member.

- **System communication**—Aircraft Controller Area Network (CAN), Ethernet, and fiber optics
- **System electromagnetic interference (EMI) mitigation and standards**—Shielding; DOD–160(RTCA, Inc., 2010) and MIL–STD–461 (Department of Defense, 2015)
- **System fault protection**—Fuse, circuit breaker, and current limiter
- **System thermal management**—Active/passive, ambient/cryogenic, and distributed/mixed

The Advanced Air Vehicle Program, Advanced Air Transport Technology Project, Hybrid Gas-Electric Power Subproject requires this test bed to meet the subproject's technology development goals for future single-aisle commercial electric aircraft. This test facility will provide a path for full-scale powertrain component development and demonstration prior to flight.

In FY17, the NASA Electric Aircraft Testbed (NEAT) was brought online to support the first powertrain testing of subscale systems for single-aisle transport hybrid electric aircraft. The testbed passed safety reviews and operations were completed for machine pairs at the 125 kilowatt and 250 kilowatt levels, validating and maturing the strategies for using electric machine pairs to emulate a turbine engine with an integrated electrical generator, and an electric motor driving a propulsive fan. These are the key building blocks for hybrid and turboelectric aircraft powertrains, which will be built and tested at successively higher power and voltage levels, and with increasingly complex architectures toward full-scale systems over the next several years.

The first full powertrain testing is currently underway. This is a subscale, simplified powertrain for NASA's 2.6 megawatt tail-cone thruster Single-Aisle Turbo-electric Aft-Boundary Layer (STARC-ABL) concept (Welstead, 2016). STARC-ABL is a lightly distributed architecture, which pulls power off of the two under-wing turbine engines and routes power through a direct current bus to the tail of the aircraft. At the tail, an electric motor then drives a propulsive fan to provide additional thrust while reducing drag by reenergizing the aircraft's aft boundary layer found at the back of the plane. The tests, which are currently underway, are working out controls, safety and electromagnetic interference issues for this design, using non-flight-weight components at 500 kilowatts and 600 Volts. Designs for a megawatt-scale powertrain with additional systems added for energy storage, fault isolation and dynamic controls will be completed in FY18 and plans are in place to begin operations in FY19.

The reconfigurable powertrain testbed is located at NASA Glenn Plum Brook Station in the recently refurbished Hypersonic Tunnel Facility (HTF) as shown in Fig. 1. The testbed is under development to support full-scale powertrain testing under actual flight scenarios that can support cryogenic fuel, high voltage, large wingspan, electromagnetic interference, and high power research hardware. Moreover, flight altitude capability is being added to support up to 50,000 feet climbing conditions within 15 minutes in a chamber large enough to include the entire powertrain. The facility also includes 12MW of 4160V three-phase power, 900 kW of water tower cooling, and a remote control room for potentially hazardous concept of operations such as liquid hydrogen. (Epstein, 2013) (Jansen, 2017) (Armstrong, 2015) (Choi, 2014) (Clarke, 2015) (Jansen, 2015) (Terorde, 2015) (Jones, 2016)

As shown in Fig. 2, the entire powertrain testbed fits within the building utilizing the exact cable lengths that would fit inside a Boeing 737-700 vehicle after being retrofitted with a tail-cone thruster.

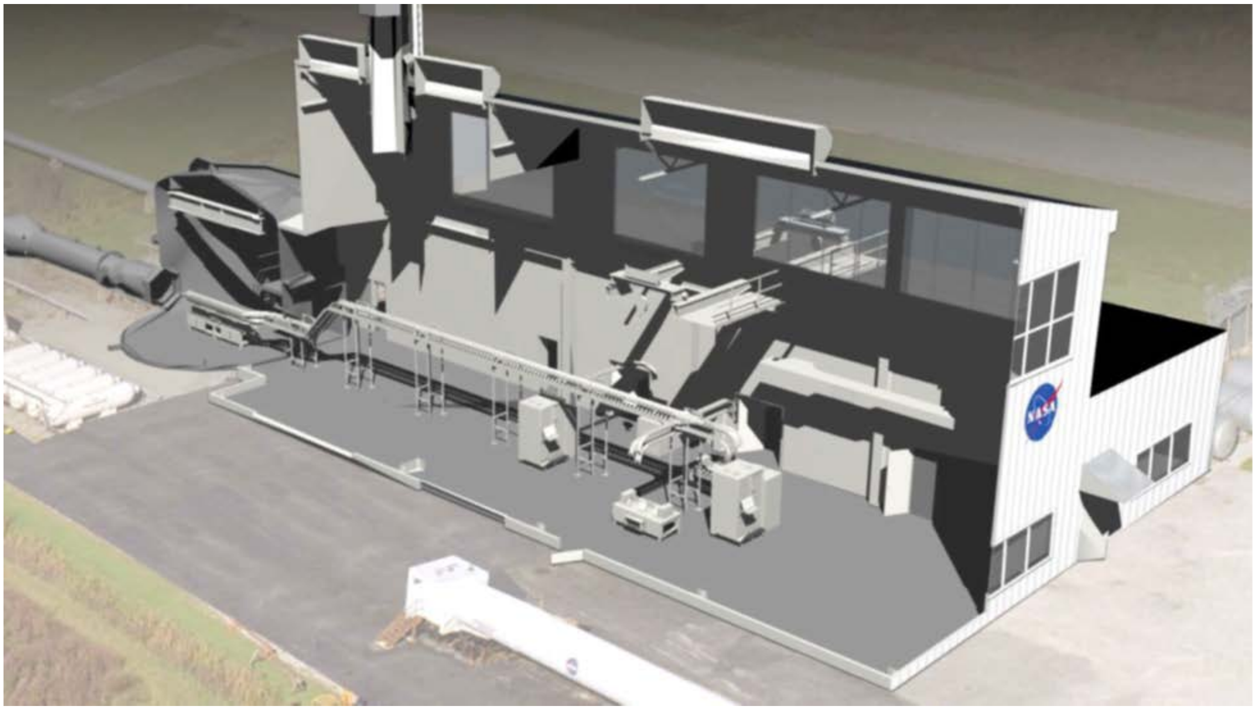

Fig. 1 NASA Electric Aircraft Testbed with STARC-ABL Configuration.

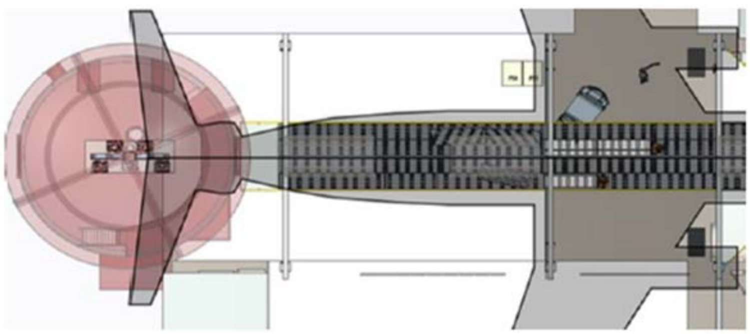

Figure 2. Top View of STARC-ABL Powertrain

III.   Basic Configuration

Shown in Fig. 3 is the basic configuration of the NEAT STARC-ABL powertrain composed of motor pairs. Note in the figure that the Green shaded machines represent the 500kW tail-cone thruster configuration that is current installed and operational, and the Yellow shaded machines are combined with the Green shaded machines to form the 1MW tail-cone thruster configuration currently under development.

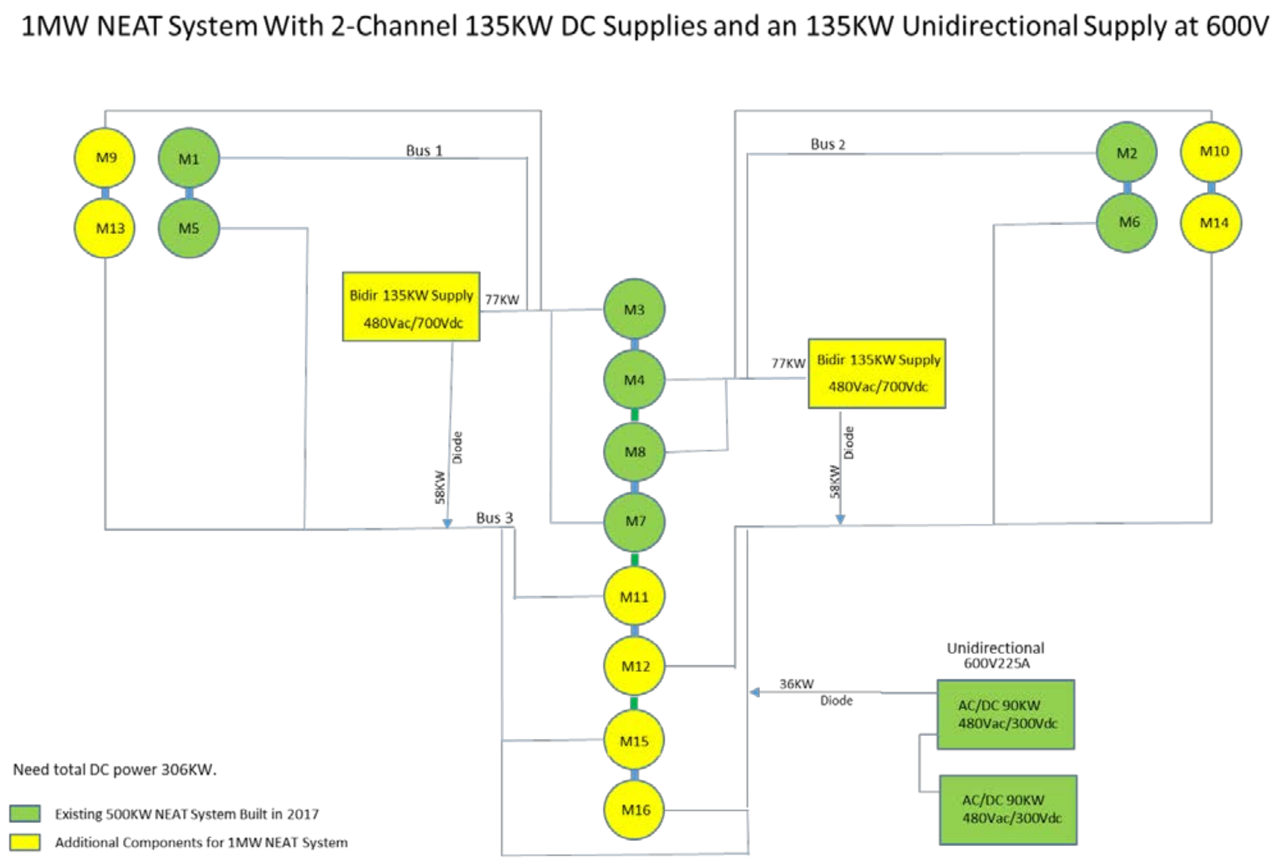

Figure 3. NEAT 1MW STARC-ABL Configuration

In Fig. 4 is the full interconnection diagram is shown including the power, communication, and fault management connections. Initially all the components are COTS sourced to provide a safe frame-work for system integration and then research components are gradually inserted into the working system. There is also a separate PLC and DAQ system to provide independent system protections and instrumentation. Also included is a water-glycol based thermal management system to provide inverter and motor cooling. The M5 and M6 motors are used to emulate turbines driving the M1 and M2 generators and represent the power extracted from the turbofans. And the M3 and M4 motors represent the tail-cone propulsor and receive their power from the turbo-generators M1 and M2. The M7 and M8 motors represent the tail-cone ducted fan and emulate the actual speed/torque curves without the need for a wind tunnel.

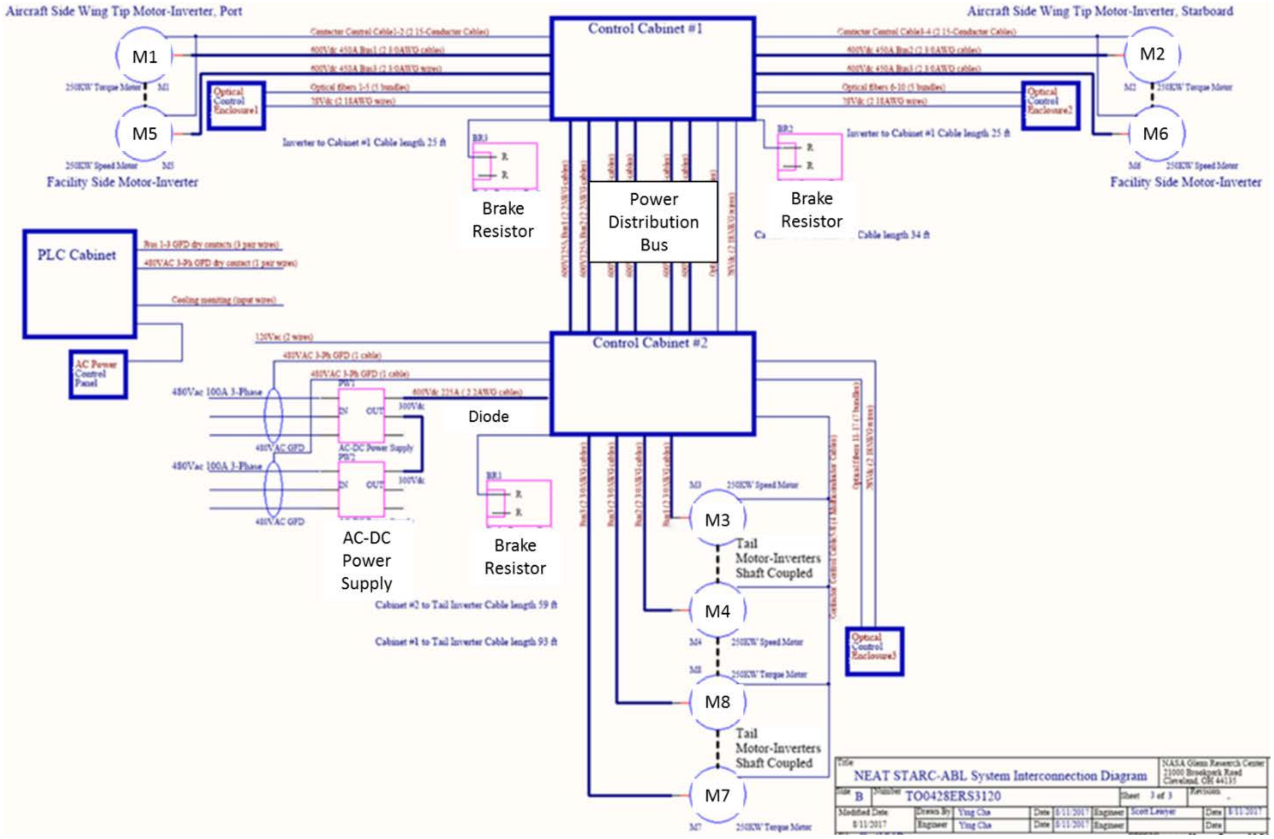

Figure 4. Full Interconnection Diagram for STARC-ABL

IV. Communication, Fault Management and Grounding

All communication is over optical fiber with data and commands based on the ARINC 664 protocol (AFDX, 2018) which use redundant communication links. Note that the braking resistors are used to provide an upper limit voltage on the aircraft power distribution bus and the diode on the power supply provides a lower limit voltage. This insures safe operation of the testbed while operating with new control systems. In addition, ground fault detection and insulation resistance detection are employed on the AC facility side and DC aircraft side to provide early warning detection capability.

As shown in Fig. 5, the aircraft powertrain communication is handled with PowerDNA units implementing the ARINC 664 protocols and all of the machine drives utilize optical CANbus. The master PowerDNA communicates via UDP to two PCs, one is used for providing flight profile controls and the other is used for inverter diagnostics. In addition, a separate instrumentation suite system is employed to independently record all communication, power, and diagnostic information during each test.

Fig. 6 shows the basic error handling information flow diagram. Note the primary safety feature is the use of COTS inverters that provide a wide range of permissives and intelligent fault response such as any communication interruption will disable the inverters. The facility is also global monitoring for any short to ground condition to disable the whole system. Each motor pair has a dedicated powerDNA providing speed and torque commands but also communicate any errors to the inverters detected from somewhere else in the powertrain. In addition, the inverters communicate any machine levels error up to the local powerDNA and then to the master powerDNA and finally to the master PC. So full supervisory control and fault detection is maintained at the master PC GUI but flight-critical safety is managed locally at the inverter hardware level. In addition, all power distribution is fused to prevent over-current faults.

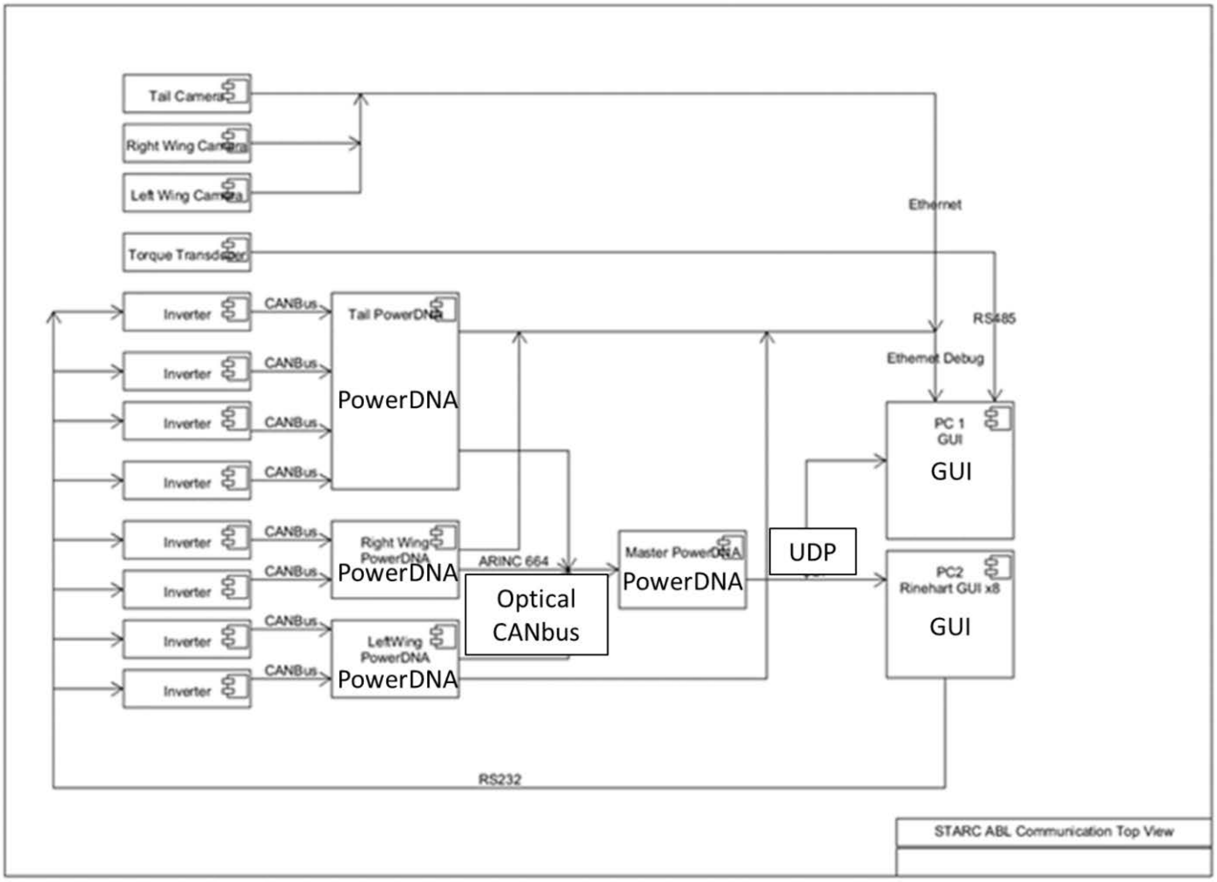

Figure 5. STARC-ABL Communication and Control

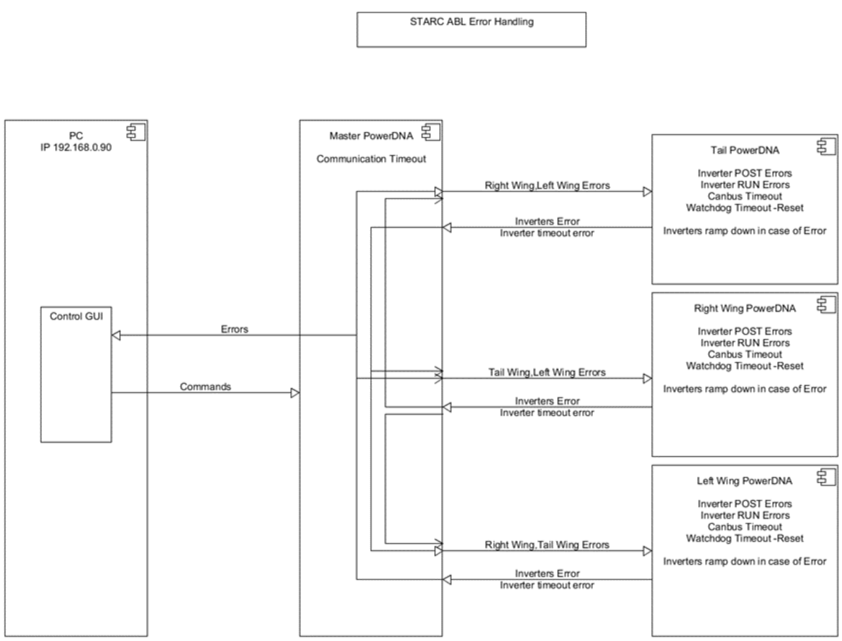

Figure 6. STARC-ABL Error Handling

Another critical safety feature is employing a fully bonded and grounded system as shown in Fig. 7. Note all structure is grounding with less than 2 milliohm bonding resistance. For this initial setup this grounding scheme is adequate to maintain safety, but is not fully reflective of an aircraft environment. In Figs. 8-9 is shown the ground fault detection scheme employed and the isolated aircraft DC bus. All current carrying power lines are shielded on both ends.

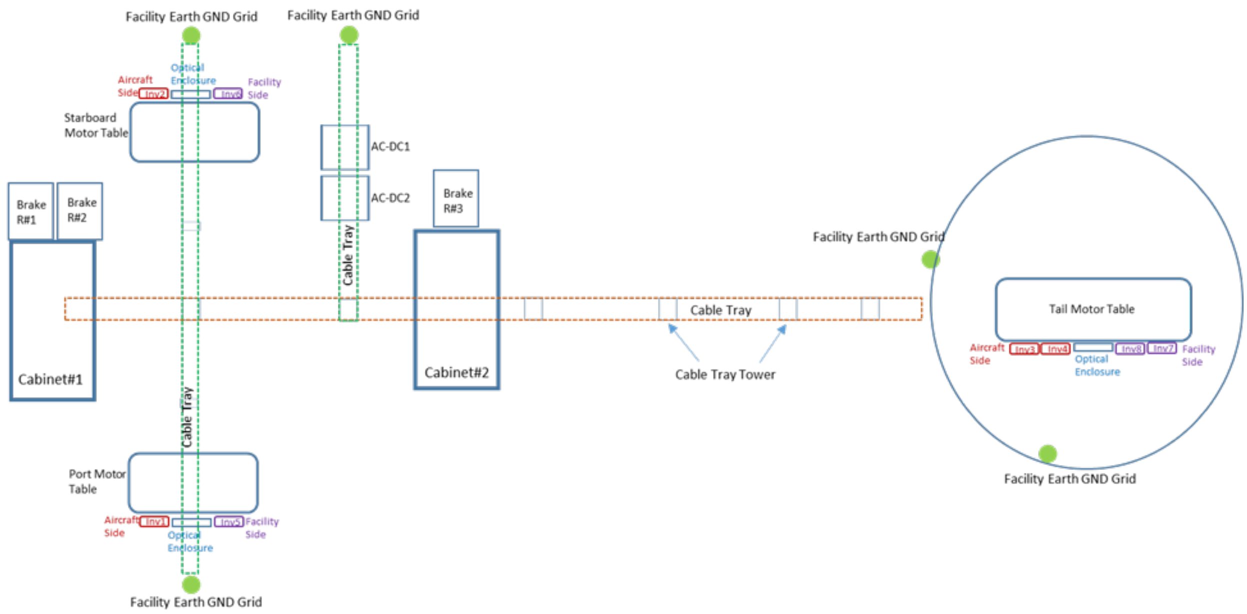

Figure 7. Current Grounding Schematic

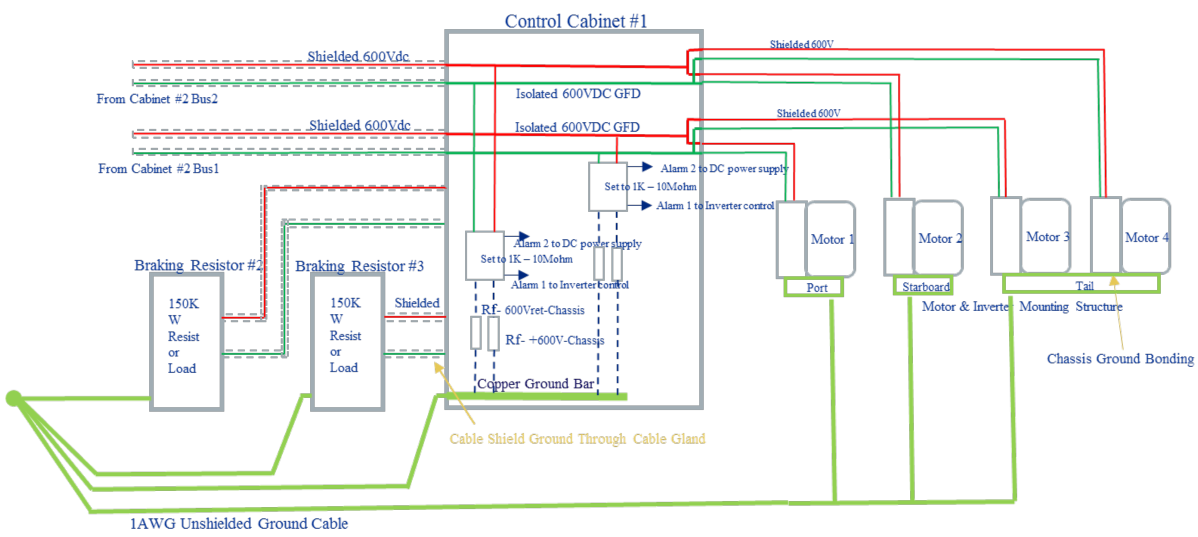

Figure 8. Cabinet #1 Fault Management and Grounding

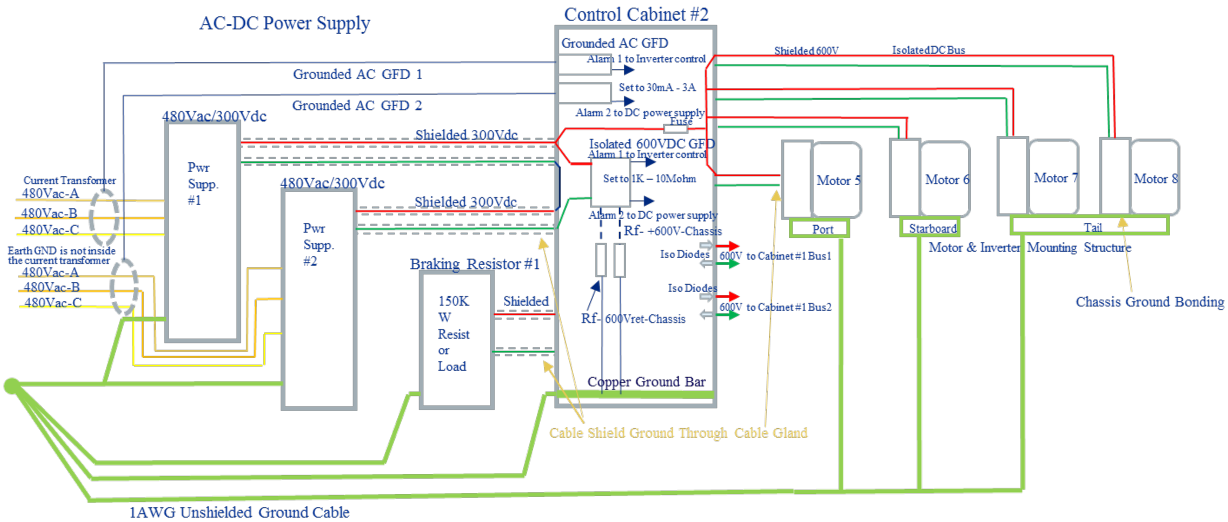

Figure 9. Cabinet #2 Fault Management and Grounding

V. NPSS Scaling to turbines and ducted fan

The Numerical Propulsion System Simulator Software was incorporated into the NEAT to enable a more realistic dynamic response that accounts for the actual turbofan and ducted fan responses. NPSS is an industry standard engine cycle model that is able to model full-scale propulsor components. The NPSS was integrated into the Matlab/Simulink environment via the S-function for a common platform with other NEAT simulation tools. A Simulink UDP library block in the NPSS Simulink Simulation is used to send and receive data from the NEAT GUI that includes:

- Inputs: Altitude, Mach/Speed, PLA/Wf, Torque Electric Generator
- Outputs: Low Pressure Shaft Speed

Initial testing was completed using a pseudo-real-time block in Matlab/Simulink and full STARC-ABL system testing was recently completed as well. This simple engine model in NPSS was interfaced to the NEAT GUI without a fuel flow controller but running in pseudo-real-time to provide approximate shaft dynamic time constants. The engine model in NPSS is being improved to more accurately include operability margins. The next step would be to enable real-time simulation of the engine in either NPSS or T-MATS to enable closed loop control of the turbofan engine with power electronics hardware. This will enable the use of FADEC flight hardware to support high fidelity engine control system interactions with the power system controller to simulate overall control architecture.

Initial validation of the modeling tools was completed utilizing a single-pair of motors as shown in Fig. 10. and highlighted in Fig. 11.

Figure 10. Initial 125kW Machine Pair Demonstration

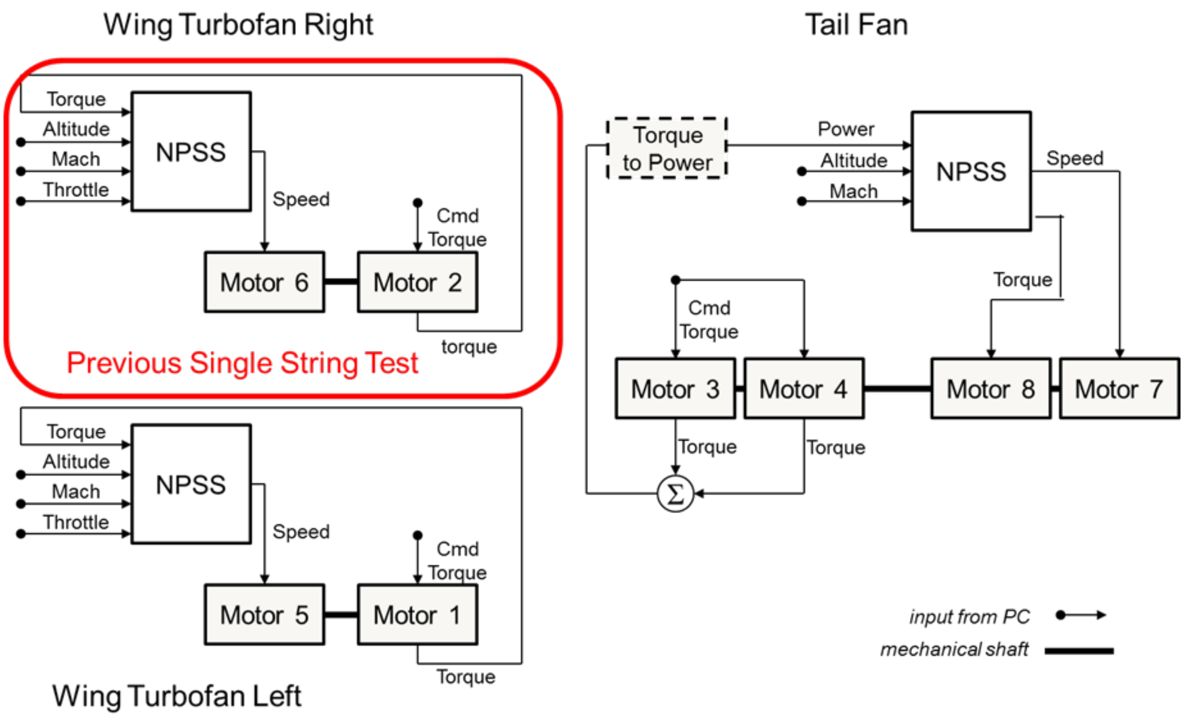

Figure 11. NPSS Control Schematic

Note in Fig. 11 that NPSS is used to provide speed commands to the turbo-generators and supplies both speed and torque commands for the simulated tail cone ducted fan motors 7 and 8.
(AFDX, 2018)
Also developed a Simulink/SimPowerSystems model of the STARC-ABL configuration of NEAT as shown in Fig. 12 that builds on the validated single-string model. It is used to analyze control schemes, operation in nominal and fault conditions, and power quality.

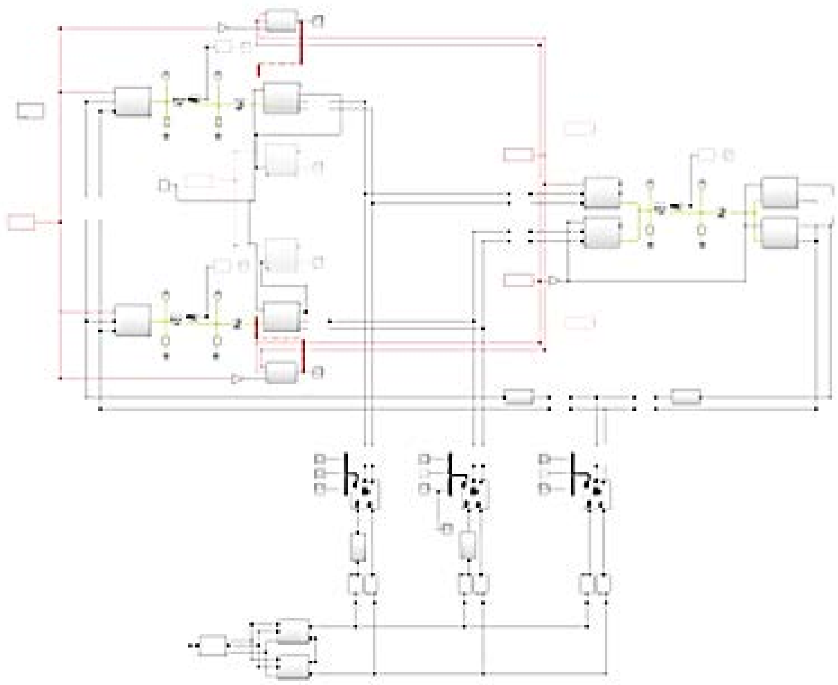

Figure 12. Dynamic Power System Model

VI. Test Results – 500kW STARC-ABL

Results from NEAT dynamic Simulink model, in STARC-ABL configuration, were compared with test data recorded at NEAT. The Simulink model used to generate results only contained NEAT electrical system and motors and did not include NPSS. The motor commands used in the simulation were the same commands sent to respective motors.

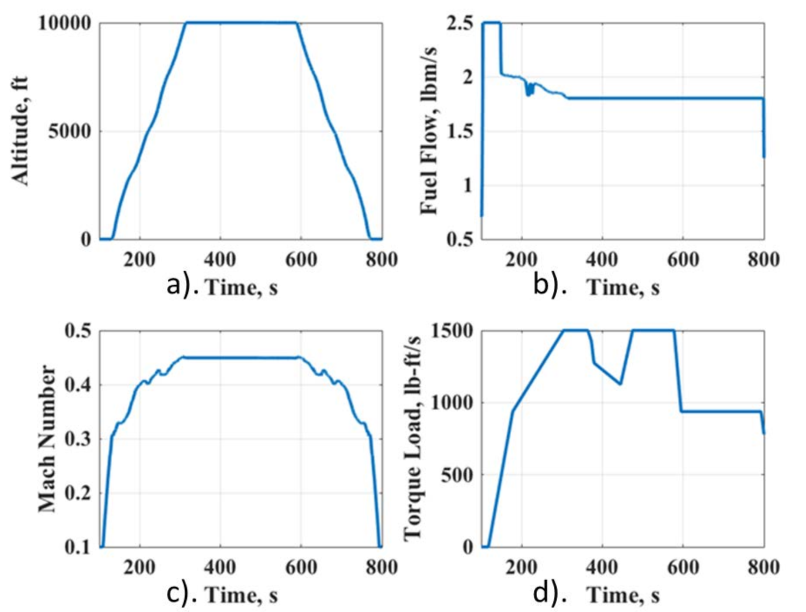

Figure 13. Flight Profile for NPSS Testing

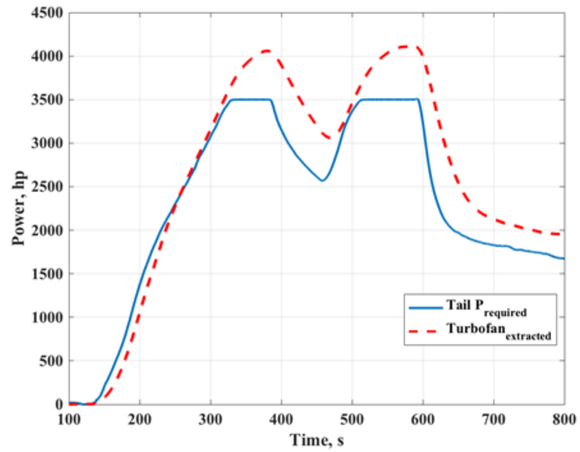

Figure 14. Power Required At Tail Fan and Turbo-Generator

The flight profile shown in Fig. 13 was used for initial NPSS testing. The NPSS inputs include the altitude, Wf, Mach number, and shaft torque. The power required by the tail fan, and the power extracted to compensate for losses in the system are provide in Fig. 14. Note the delay in the transient extraction off of the turbofans due to torque filtering. (Connolly, 2018). In the future the turbo-generator will utilize voltage control instead of speed or torque control to naturally balance the tail-cone thruster power with the generated power.

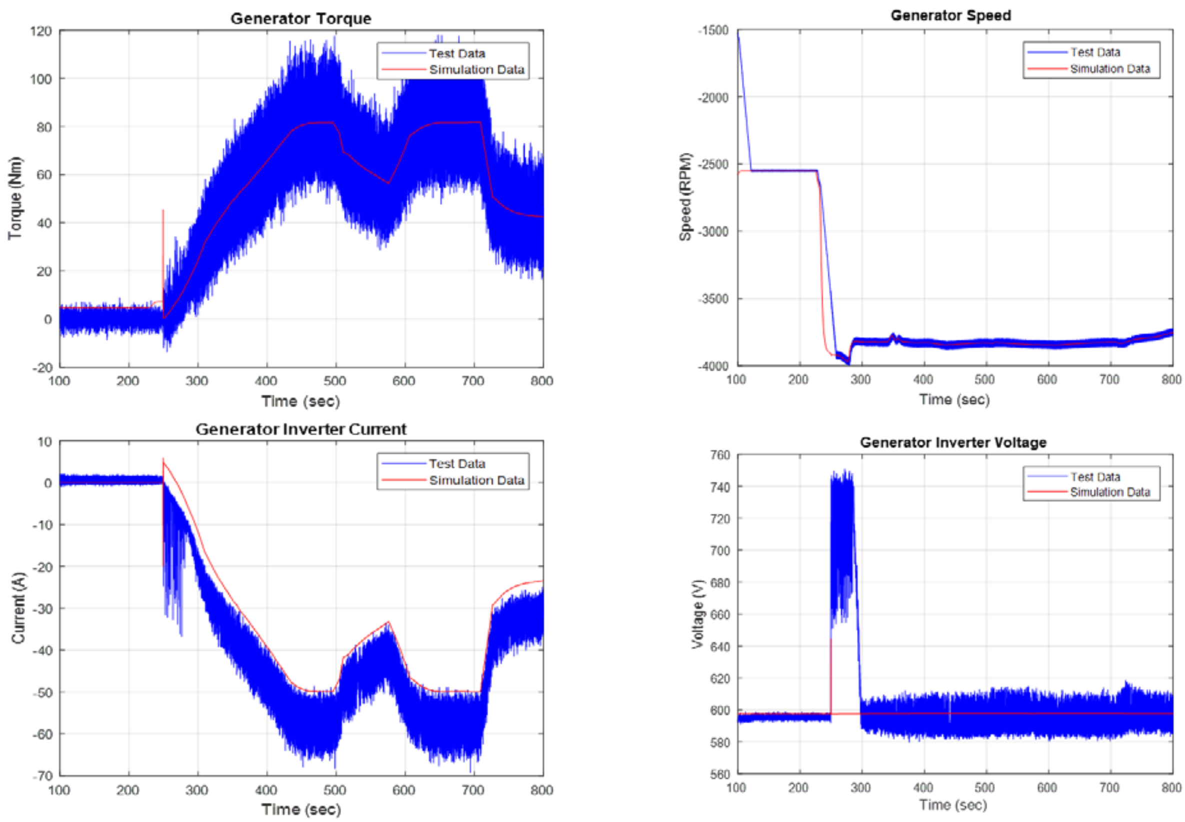

Figure 15. Generator M1 Model Validation

Initial test results indicate very good agreement with model predictions for both the generator M1 shown in Fig. 15 and the tail-cone propulsor shown in Fig. 16. Note that the predominant error was during short startup transients but for the vast majority of the flight profile we see excellent agreement.

Most recently, NEAT was successfully operated with the full 900 NM flight profile indicated in Fig. 17. This flight profile extended beyond 2 hours and fully tested all the integrated systems. The power budget of the system is found in the appendix. The challenges with operating this full profile included:

- Thermally managing the extended duration test
- Addressing EMI between the controls and inverter
- Load balancing the system due to millisecond communication delays between turbo-generators
- Minimizing bus transients/power quality improvement without adding bus energy storage and regenerating
- Fault management/buffering issues with a complex system

Full recorded results are available of this initial profile and additional post-processing of the data will be used to improve the powertrain fault and control systems. But this initial test indicates the 500kW STARC-ABL powertrain can be operated under a realistic flight profile utilizing COTS equipment. Powertrain operation and flight profile details are found in the Appendix.

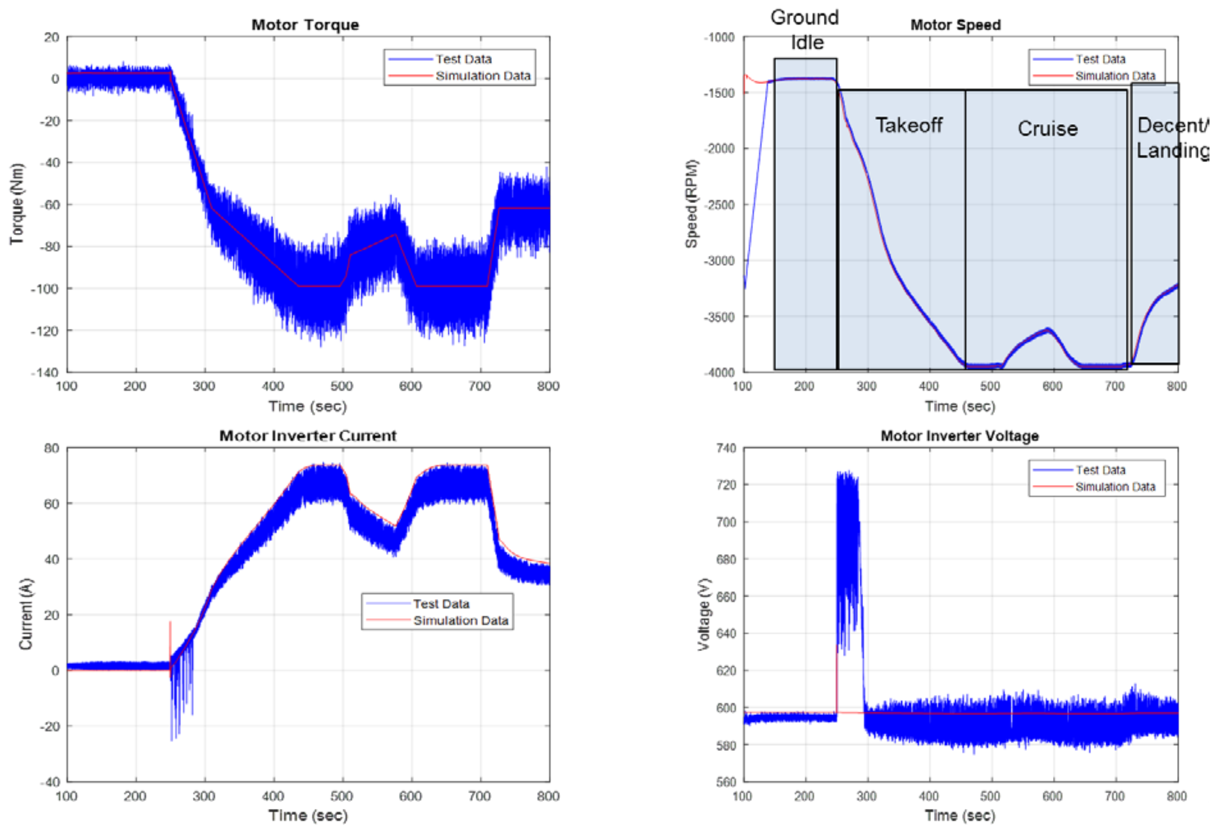

Figure 16. Motor M3 Model Validation

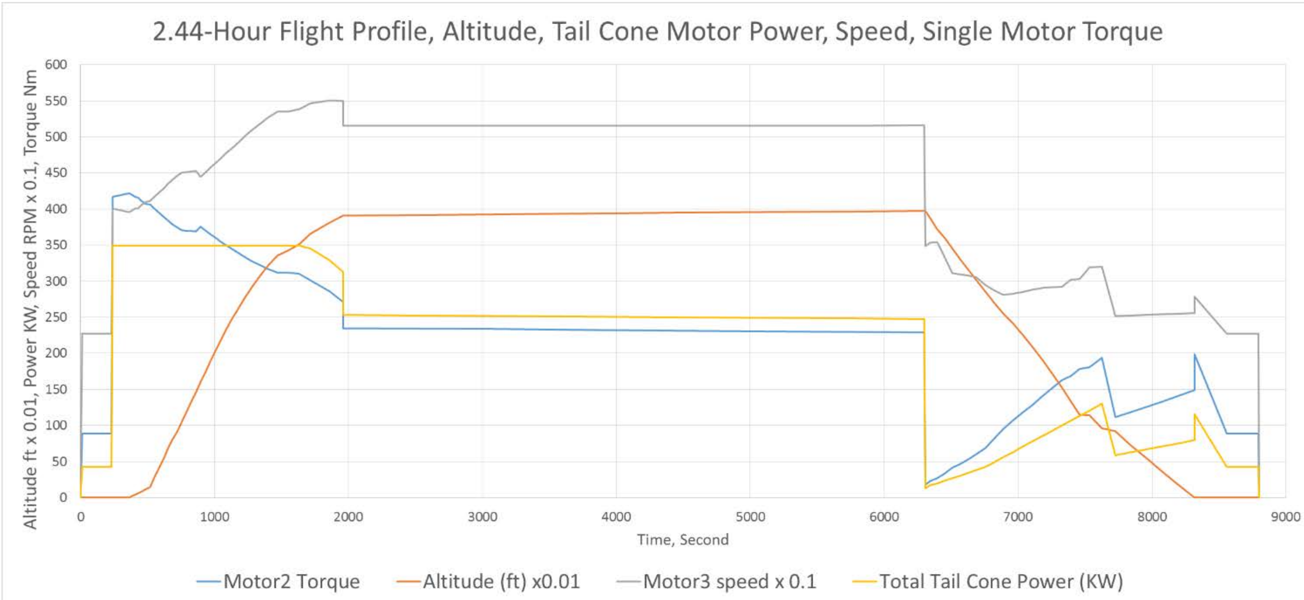

Figure 17. NEAT STARC-ABL Powertrain Testing for 900 NM Flight Profile

VII. Lessons Learned and Next Steps

.

The build-up of a complex electric aircraft powertrain requires integrating power, propulsion, and thermal components with sufficient control and fault response to protect full-scale, high power, high value research hardware. The simplest building block is based on the single-string as shown in Fig. 10 comprised of two shaft connected machine operating as a turbine-generator or propulsor-ducted fan combination. Some of the lessons learned include:

- EMI shielding is critical for safe and proper operation of the powertrain even with DO-160G compatible equipment
- Federated fault response with localized feedback/controls are important for orderly shutdown sequencing
- Electric machines can be scaled and controlled to simulate a turbine and ducted fan operation
- System interactions between components must be tested to account for common modes, grounding loops, electrical and mechanical resonant conditions
- Spline coupling selection impacts controllability
- Turbine and Electric Powertrain modeling can be very accurate if the component controls are fully characterized
- Optical fiber and digital instrumentation are required for robust communication and sensors
- Higher voltage and current present new issues such as insulation resistance breakdown and power quality challenges when operating near rated equipment limits
- Torque measurements are effected by cogging, EMI, torsional resonance, spline back-lash, and acquisition rates
- Shielding throughout the powertrain limits the ability to acquire data from transducers forcing calculated results via inverter software measurements.

The next steps of NEAT development are shown in Figs. 18-19. First, we successfully completed the single-string test in FY17 (shown in Fig. 10). Next we built and successfully tested the STARC-ABL configuration with a 500kW tail-cone thruster. Our next steps include doubling the tail-cone thruster power to 1MW, adding triple control redundancy, adding smart energy storage, incorporate complete closed loop engine control with fan speed feedback to enable real-time turbine and fan emulation, and beginning to address proper aircraft grounding.

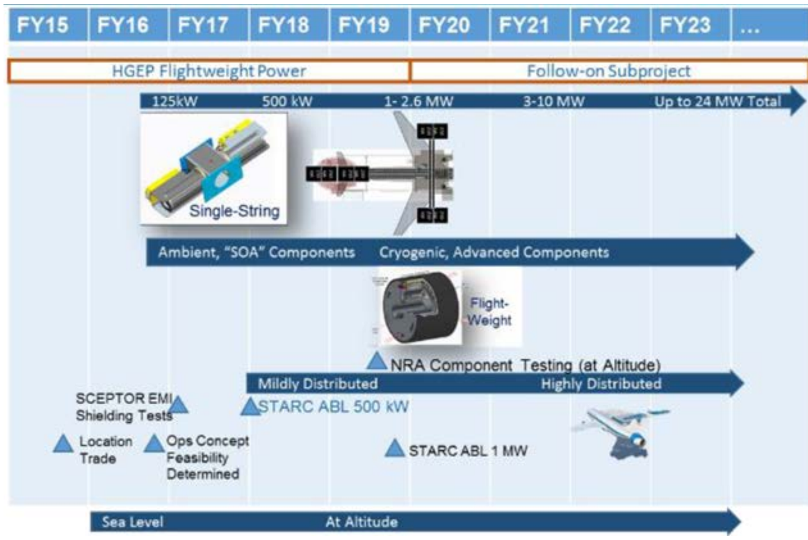

Figure 18. Research Plan

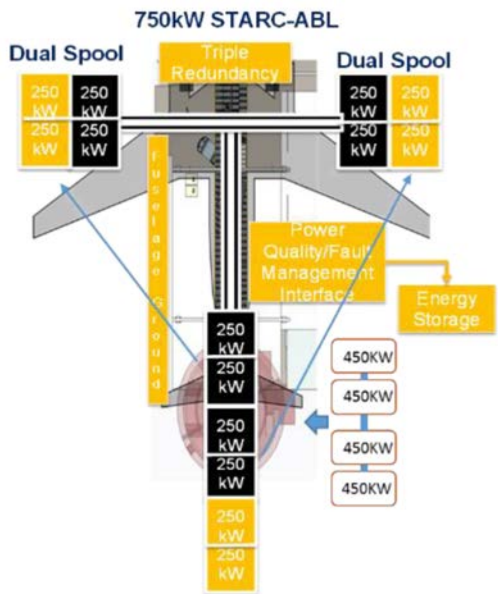

Figure19. Incorporating Flight Readiness

VIII. Conclusion

Full-scale electric aircraft testing is important because of the EMI, thermal management, cable impedance, fault response, and high voltage effects on the performance of the powertrain. A novel approach that utilizes a regenerative power strategy with machine pairs that emulate in real-time the turbine and propulsors was presented. A full 900 NM flight-profile was successfully demonstrated at NEAT. Initial results indicate the importance of a smart fault management/energy storage component on the DC bus in addition to managing EMI and grounding challenges. The next steps are to increase the power level and incorporate flight-readiness features such as proper fuselage grounding, triple control redundancy, dual spool power extraction, and intelligent fault management.

Appendix

Table 1. STARC-ABL Power Budget

0.5MW Wing Tip Speed Motor Shaft Power	<<	0.5MW Wing Tip Speed Motor Input Power	<<	0.5MW Wing Tip Speed Inverter Input Power	<<	0.5MW Wing Tip Speed Inverter Input Power		0.5MW Wing Tip Torque Motor Output Power	>>	0.5MW Wing Tip Torque Inverter Output Power	>>	2 x 0.5MW Wing Tip Torque Inverter Output Power		
0.5MW Tail Speed Inverter Output Power	>>	0.5MW Tail Speed Motor Shaft Power	>>	0.5MW Tail Torque Motor Output Power	>>	0.5MW Tail Torque Inverter Output Power	>>	2 x 0.5MW Tail Torque Inverter Output Power		DC Power Supply Output Power				
	0.5MW Wing Tip Speed Motor				Inverter (DC to 3-Phase AC)			Wire Loss (DC Supply to Inverter)@50°C					Total Wing Tip Speed Inverter Input Power w/	2 x Wing Tip Inverter Input Power (KW)
DC Link Voltage (V)	Max Power Output at Motor Shaft (W)	Efficiency	Power Loss (W)	Motor Input Power (W)	Efficiency	Power Loss (W)	Input Power (W)	4/0 AWG Total 30 feet (W)	Voltage Drop (V)	3/0 AWG Total 30 feet (W)	Voltage Drop (V)	DC Link Current at Max Power (A)		
700	500,000	0.98	10,204	510,204	0.98	10,412	520,616	909	1.22	1147	1.54	744	522	1043.1
	0.5MW Wing Tip Torque Motor				Inverter (3-Phase AC to DC)			Wire Loss (Inverter to DC Supply)@50°C				DC Output Current at Max Power (A)	Total Torque Inverter Output Power w/	2 x Torque Inverter Output Power (KW)
DC Link Voltage (V)	Max Shaft Input Power (W)	Efficiency	Power Loss (W)	Motor Output Power (W)	Efficiency	Power Loss (W)	Output Power (W)	4/0 AWG Total 30 feet (W)	Voltage Drop (V)	3/0 AWG Total 30 feet (W)	Voltage Drop (V)			
700	500,000	0.98	10,000	490,000	0.98	9,800	480,200	774	1.13	975	1.42	686	479	958.9
	0.5MW Tail Speed Motor				Tail Speed Inverter (DC to 3-			Wire Loss (DC Supply to Inverter)@50°C					Total Tail Speed Inverter Input Power w/ 4/0 AWG wire (KW)	2 x Tail Speed Inverter Input Power (KW)
DC Link Voltage (V)	Max Power Output at Motor Shaft (KW)	Efficiency	Power Loss (KW)		Efficiency	Power Loss (KW)	Output Power (KW)	4/0 AWG Total 30 feet (W)	Voltage Drop (V)	3/0 AWG Total 30 feet (W)	Voltage Drop (V)	DC Input Current at Max Power (A)		
700	460	0.98	9		0.98	10	470	771	1.13	972	1.42	685	479	958.9
	0.5MW Tail Torque Motor				Torque Inverter (3-Phase AC to			Wire Loss (Inverter to DC Supply)@50°C				DC Output Current at Max Power (A)	Total Torque Inverter Output Power w/	2 x Torque Inverter Output Power (KW)
DC Link Voltage (V)	Max Shaft Input Power (KW)	Efficiency	Power Loss (KW)	Motor Output Power (KW)	Efficiency	Power Loss (KW)	Output Power (KW)	4/0 AWG Total 30 feet (W)	Voltage Drop (V)	3/0 AWG Total 30 feet (W)	Voltage Drop (V)			
700	460	0.98	9	451	0.98	9	442	656	1.04	827	1.31	632	442	883.1
1MW System:														
Tail Torque Inverter Output Power (KW)	wing Tip Speed Inverter Input Power (KW)	Power Need from DC Power Supply (KW)	DC Link Input Current (A)		AC-DC Power Supply Efficiency	AC Input Power (KW)	480Vac Phase Current (A)	DC Link Voltage (V)						
883	1,043	160	228.5		0.85	188.2	226.4	700						

Table 2. STARC-ABL 900 NM Flight Profile

Flight Segment	Time (min)	Altitude (ft)	Mach	Fuel Flow (lbs/hr)	Onboard Fuel (lbs)	Net Thrust (lbs)	Tail Cone Power (HP)
Taxi	0	0	0.0000	765	8793	1171	422
	4	0	0.0000	765	8742	1171	422
Takeoff	4	0	0.0000	9540	8742	9293	3500
	6	0	0.3000	9540	8424	28795	3500
Segment 1 Climb	6	0	0.3000	9946	8424	28795	3500
	6.34	190	0.3177	9426	8368	26445	3500
	6.71	396	0.4806	9161	8311	19562	3500
	7.11	620	0.4918	8944	8251	19092	3500
	7.53	854	0.6000	8663	8189	18811	3500
	8.04	1139	0.6595	8489	8117	18371	3500
	8.61	1457	0.6649	8387	8037	18104	3500
	9.17	2766	0.6702	8265	7958	17808	3500
	9.74	4086	0.6751	8125	7881	17484	3500
	10.3	5415	0.6797	7966	7806	17131	3500
	10.86	6755	0.6840	7789	7732	16749	3500
	11.43	8108	0.6878	7593	7660	16340	3500
	12	9153	0.7031	7475	7588	16250	3500
	12.58	10518	0.7067	7178	7517	15827	3500
	13.16	11883	0.7103	6949	7448	15428	3500
	13.75	13249	0.7139	6721	7381	15055	3500
	14.34	14614	0.7177	6488	7316	14708	3500
	14.94	16017	0.7200	6257	7253	14321	3500
	15.55	17484	0.7200	6043	7191	13833	3500
	16.17	18950	0.7200	5830	7129	13345	3500
	16.8	20417	0.7200	5617	7068	12857	3500
	17.47	21883	0.7200	5404	7008	12369	3500
	18.16	23349	0.7200	5191	6947	11881	3500
	18.88	24816	0.7200	4977	6885	11393	3500
	19.65	26282	0.7200	4764	6823	10905	3500
	20.47	27748	0.7200	4551	6759	10417	3500
	21.34	29215	0.7200	4338	6695	9929	3500
	22.29	30681	0.7200	4125	6628	9441	3500
	23.32	32147	0.7200	3911	6559	8953	3500
	24.47	33568	0.7220	3704	6486	8473	3500
	25.76	34181	0.7582	3630	6407	8250	3500
	27.19	35094	0.7812	3581	6321	8106	3498
Segment 2 Climb	27.19	35094	0.7812	3581	6321	8106	3498
	28.57	36529	0.7750	3426	6241	7732	3457
	30.97	38117	0.7850	3232	6107	7250	3296
	32.63	39116	0.7850	3071	6020	6876	3130
Cruise	32.63	39116	0.7850	2441	6020	5534	2538
	51.49	39273	0.7850	2428	5255	5500	2522
	73.8	39463	0.7850	2412	4355	5460	2503
	96.26	39656	0.7850	2397	3455	5420	2485
	104.96	39732	0.7850	2391	3108	5404	2478
Descent	104.96	39732	0.7850	412	3108	0	129
	105.71	38783	0.7553	431	3103	0	169
	106.6	37255	0.7422	439	3096	0	198
	107.52	35976	0.7164	465	3089	0	234
	108.47	34522	0.6944	487	3082	0	270
	109.45	33051	0.6731	509	3074	0	303
	110.46	31603	0.6505	535	3065	0	344
	111.5	30121	0.6294	559	3055	0	385
	112.58	28554	0.6124	583	3045	0	426
	113.68	27078	0.5907	618	3034	0	492
	114.81	25503	0.5739	654	3022	0	560
	115.99	24171	0.5440	713	3009	0	632
	117.22	22529	0.5306	754	2994	0	706
	118.47	20887	0.5171	804	2977	0	782
	119.72	19026	0.5160	844	2960	0	857
	120.93	17146	0.5160	883	2943	0	930
	122.1	15265	0.5160	922	2925	0	1001
	123.22	13385	0.5160	974	2907	0	1069
	124.29	11504	0.5160	1028	2889	0	1134
	125.55	11442	0.4099	1290	2865	0	1210
	127.09	9587	0.4099	1375	2831	0	1303
	128.76	9179	0.3000	623	2803	0	589
	130.62	7344	0.3000	645	2784	0	627
	132.55	5508	0.3000	667	2762	0	666
	134.53	3672	0.3000	705	2740	0	708
	136.55	1836	0.3000	750	2715	0	752
	138.6	0	0.3000	796	2689	0	798
Approach	138.6	0	0.3000	1889	2689	1889	1159
	142.6	0	0.0000	1171	2587	1171	422
Taxi	142.6	0	0.0000	765	2587	1171	422
	146.6	0	0.0000	765	2536	1171	422

Table 3. Scaled Profile Successfully Operated

Flight Segment	Time (Sec)	Altitude (ft)	13.4% of Tail Cone Power (KW)	10% of Tail Cone Power (KW)	Tail Motor Speed, 2:1 of Fan Speed (RPM)	Tail Cone Motor Torque, per motor (Nm)	Motor1 Torque	Motor2 Torque	Motor3 speed	Motor4 torque	Motor5 Speed	Motor6 Speed	Motor7 torque	Motor8 torque
Startup	**0**	**0**	0	0	0	0	**0**	**0**	**0**	**0**	**0**	**0**	**0**	**0**
Taxi	10	0	42	31	2269	66	**66**	**66**	**2269**	**-66**	**2269**	**2269**	**66**	**-66**
	230	0	42	31	2269	66	**66**	**66**	**2269**	**-66**	**2269**	**2269**	**66**	**-66**
Takeoff	240	0	350	261	4004	311	**311**	**311**	**4004**	**-311**	**4004**	**4004**	**311**	**-311**
Segment 1 Climb	360	0	350	261	3955	315	**315**	**315**	**3955**	**-315**	**3955**	**3955**	**315**	**-315**
	380	190	350	261	3974	314	**314**	**314**	**3974**	**-314**	**3974**	**3974**	**314**	**-314**
	403	396	350	261	4007	311	**311**	**311**	**4007**	**-311**	**4007**	**4007**	**311**	**-311**
	427	620	350	261	4011	311	**311**	**311**	**4011**	**-311**	**4011**	**4011**	**311**	**-311**
	452	854	350	261	4058	307	**307**	**307**	**4058**	**-307**	**4058**	**4058**	**307**	**-307**
	482	1139	350	261	4097	304	**304**	**304**	**4097**	**-304**	**4097**	**4097**	**304**	**-304**
	517	1457	350	261	4112	303	**303**	**303**	**4112**	**-303**	**4112**	**4112**	**303**	**-303**
	550	2766	350	261	4168	299	**299**	**299**	**4168**	**-299**	**4168**	**4168**	**299**	**-299**
	584	4086	350	261	4226	295	**295**	**295**	**4226**	**-295**	**4226**	**4226**	**295**	**-295**
	618	5415	350	261	4285	291	**291**	**291**	**4285**	**-291**	**4285**	**4285**	**291**	**-291**
	652	6755	350	261	4347	287	**287**	**287**	**4347**	**-287**	**4347**	**4347**	**287**	**-287**
	686	8108	350	261	4407	283	**283**	**283**	**4407**	**-283**	**4407**	**4407**	**283**	**-283**
	720	9153	350	261	4461	279	**279**	**279**	**4461**	**-279**	**4461**	**4461**	**279**	**-279**
	755	10518	350	261	4502	277	**277**	**277**	**4502**	**-277**	**4502**	**4502**	**277**	**-277**
	790	11883	350	261	4511	276	**276**	**276**	**4511**	**-276**	**4511**	**4511**	**276**	**-276**
	825	13249	350	261	4520	276	**276**	**276**	**4520**	**-276**	**4520**	**4520**	**276**	**-276**
	860	14614	350	261	4528	275	**275**	**275**	**4528**	**-275**	**4528**	**4528**	**275**	**-275**
	896	16017	350	261	4450	280	**280**	**280**	**4450**	**-280**	**4450**	**4450**	**280**	**-280**
	933	17484	350	261	4513	276	**276**	**276**	**4513**	**-276**	**4513**	**4513**	**276**	**-276**
	970	18950	350	261	4575	272	**272**	**272**	**4575**	**-272**	**4575**	**4575**	**272**	**-272**
	1008	20417	350	261	4639	269	**269**	**269**	**4639**	**-269**	**4639**	**4639**	**269**	**-269**
	1048	21883	350	261	4710	265	**265**	**265**	**4710**	**-265**	**4710**	**4710**	**265**	**-265**
	1090	23349	350	261	4779	261	**261**	**261**	**4779**	**-261**	**4779**	**4779**	**261**	**-261**
	1133	24816	350	261	4848	257	**257**	**257**	**4848**	**-257**	**4848**	**4848**	**257**	**-257**
	1179	26282	350	261	4930	253	**253**	**253**	**4930**	**-253**	**4930**	**4930**	**253**	**-253**
	1228	27748	350	261	5013	249	**249**	**249**	**5013**	**-249**	**5013**	**5013**	**249**	**-249**
	1280	29215	350	261	5095	245	**245**	**245**	**5095**	**-245**	**5095**	**5095**	**245**	**-245**
	1337	30681	350	261	5180	241	**241**	**241**	**5180**	**-241**	**5180**	**5180**	**241**	**-241**
	1399	32147	350	261	5270	236	**236**	**236**	**5270**	**-236**	**5270**	**5270**	**236**	**-236**
	1468	33568	350	261	5354	233	**233**	**233**	**5354**	**-233**	**5354**	**5354**	**233**	**-233**
	1546	34181	350	261	5355	233	**233**	**233**	**5355**	**-233**	**5355**	**5355**	**233**	**-233**
	1629	35094	350	261	5384	231	**231**	**231**	**5384**	**-231**	**5384**	**5384**	**231**	**-231**
Segment 2 Climb	1631	35094	350	261	5384	231	**231**	**231**	**5384**	**-231**	**5384**	**5384**	**231**	**-231**
	1714	36529	345	258	5466	225	**225**	**225**	**5466**	**-225**	**5466**	**5466**	**225**	**-225**
	1858	38117	329	246	5503	213	**213**	**213**	**5503**	**-213**	**5503**	**5503**	**213**	**-213**
	1958	39116	313	233	5497	203	**203**	**203**	**5497**	**-203**	**5497**	**5497**	**203**	**-203**
Cruise	1960	39116	254	189	5153	175	**175**	**175**	**5153**	**-175**	**5153**	**5153**	**175**	**-175**
	3089	39273	252	188	5154	174	**174**	**174**	**5154**	**-174**	**5154**	**5154**	**174**	**-174**
	4428	39463	250	187	5156	173	**173**	**173**	**5156**	**-173**	**5156**	**5156**	**173**	**-173**
	5776	39656	248	185	5158	172	**172**	**172**	**5158**	**-172**	**5158**	**5158**	**172**	**-172**
	6298	39732	248	185	5160	171	**171**	**171**	**5160**	**-171**	**5160**	**5160**	**171**	**-171**
Descent	6308	39732	13	10	3487	13	**13**	**13**	**3487**	**-13**	**3487**	**3487**	**13**	**-13**
	6343	38783	17	13	3534	17	**17**	**17**	**3534**	**-17**	**3534**	**3534**	**17**	**-17**
	6396	37255	20	15	3546	20	**20**	**20**	**3546**	**-20**	**3546**	**3546**	**20**	**-20**
	6451	35976	23	17	3330	25	**25**	**25**	**3330**	**-25**	**3330**	**3330**	**25**	**-25**
	6508	34522	27	20	3113	31	**31**	**31**	**3113**	**-31**	**3113**	**3113**	**31**	**-31**
	6567	33051	30	23	3095	35	**35**	**35**	**3095**	**-35**	**3095**	**3095**	**35**	**-35**
	6628	31603	34	26	3076	40	**40**	**40**	**3076**	**-40**	**3076**	**3076**	**40**	**-40**
	6690	30121	38	29	3057	45	**45**	**45**	**3057**	**-45**	**3057**	**3057**	**45**	**-45**
	6755	28554	43	32	2952	51	**51**	**51**	**2952**	**-51**	**2952**	**2952**	**51**	**-51**
	6821	27078	49	37	2873	61	**61**	**61**	**2873**	**-61**	**2873**	**2873**	**61**	**-61**
	6889	25503	56	42	2807	71	**71**	**71**	**2807**	**-71**	**2807**	**2807**	**71**	**-71**
	6959	24171	63	47	2829	79	**79**	**79**	**2829**	**-79**	**2829**	**2829**	**79**	**-79**
	7033	22529	71	53	2850	88	**88**	**88**	**2850**	**-88**	**2850**	**2850**	**88**	**-88**
	7108	20887	78	58	2887	96	**96**	**96**	**2887**	**-96**	**2887**	**2887**	**96**	**-96**
	7183	19026	86	64	2910	105	**105**	**105**	**2910**	**-105**	**2910**	**2910**	**105**	**-105**
	7256	17146	93	69	2919	113	**113**	**113**	**2919**	**-113**	**2919**	**2919**	**113**	**-113**
	7326	15265	100	75	2928	122	**122**	**122**	**2928**	**-122**	**2928**	**2928**	**122**	**-122**
	7393	13385	107	80	3020	126	**126**	**126**	**3020**	**-126**	**3020**	**3020**	**126**	**-126**
	7457	11504	113	85	3028	133	**133**	**133**	**3028**	**-133**	**3028**	**3028**	**133**	**-133**
	7533	11442	121	90	3192	135	**135**	**135**	**3192**	**-135**	**3192**	**3192**	**135**	**-135**
	7625	9587	130	97	3203	145	**145**	**145**	**3203**	**-145**	**3203**	**3203**	**145**	**-145**
	7726	9179	59	44	2517	83	**83**	**83**	**2517**	**-83**	**2517**	**2517**	**83**	**-83**
	7837	7344	63	47	2525	88	**88**	**88**	**2525**	**-88**	**2525**	**2525**	**88**	**-88**
	7953	5508	67	50	2532	94	**94**	**94**	**2532**	**-94**	**2532**	**2532**	**94**	**-94**
	8072	3672	71	53	2540	99	**99**	**99**	**2540**	**-99**	**2540**	**2540**	**99**	**-99**
	8193	1836	75	56	2548	105	**105**	**105**	**2548**	**-105**	**2548**	**2548**	**105**	**-105**
	8316	0	80	59	2556	111	**111**	**111**	**2556**	**-111**	**2556**	**2556**	**111**	**-111**
Approach	8318	0	116	86	2784	148	**148**	**148**	**2784**	**-148**	**2784**	**2784**	**148**	**-148**
Taxi	8556	0	42	31	2269	66	**66**	**66**	**2269**	**-66**	**2269**	**2269**	**66**	**-66**
	8796	0	42	31	2269	66	**66**	**66**	**2269**	**-66**	**2269**	**2269**	**66**	**-66**
Shutdown	8801	0	0	0	0	0	**0**	**0**	0	**0**	**0**	**0**	**0**	**0**

Acknowledgments

The author would like to thank Don Simon, Joe Connolly, Keith Hunker, Ralph Jansen, Cheryl Bowman, Amy Jankovsky, Gerald Hill, VPL staff, and TFOME staff, for making this work possible. *In addition this work was financially supported by the Advanced Air Transportation Technology Project/Hybrid Gas Electric Propulsion Sub-project.*

IX. References

AFDX, 2018. *Avionics Full Duplex Switched Ethernet.* [Online]
Available at: https://en.wikipedia.org/wiki/Avionics_Full-Duplex_Switched_Ethernet

Armstrong, M., 2015. *Superconducting Turboelectric Distributed Aircraft Propulsion.* Tucson, s.n.

Choi, B., 2014. *Propulsion Electric Grid Simulator (PEGS) for Future Turboelectric Distributed Propulsion Aircraft,* Cleveland: NASA.

Clarke, S., 2015. *Enabled Electric Propulsion For Flight - Hybrid Electric Aircraft Research at AFRC.,* s.l.: s.n.

Connolly, J. a. H. K., 2018. *STARC-ABL Preliminary Sim Results.* s.l.:Personal Communication.

Dyson, R., 2016. *NASA Electric Aircraft Testbed (NEAT) Development Pan - Design, Fabrication, Installation,* Cleveland: NASA/TM-2016-219085.

Dyson, R., 2017. *Precious Metal,* s.l.: Aerospace Testig International.

Epstein, A., 2013. *Aeropropulsion for Commercial Aviation in the 21st Century and Research Directions Needed.* s.l., AIAA.

Jansen, R., 2015. *Turboelectric Aircraft Drive Key Performance Parameters and Functional Requirements.* s.l., AIAA.

Jansen, R. e. a., 2017. *Overview of NASA Electrified Aircraft Propulsion (EAP) Research for Large Subsonic Transports.* Atlanta, AIAA/SAE/ASEE.

Jones, C., 2016. Electrical Model of Carbon Fibre Reinforced Polymers for the Development of Electrical Protection Systems for More Electric Aircraft.

Jones, C. N. P., 2016. *Electrical Model of Carbon Fibre Reinforced Polymers for the Development of Electrical Protection Systems for More-Electric Aircraft,* s.l.: EPE.

Moffit, B., 2017. *Analysis and Testing of Boundary-Layer-Ingesting Pusher Propeller for High Speed Rotorcraft,* Fort Worth: AHS International.

Terorde, M., 2015. Phase Balancing for Aircraft Electrical Distribution Systems. *IEEE Transactions on Aerospace and Electronics Systems,* pp. Vol. 51, No. 3.

Welstead, J. a. F. J., 2016. *Conceptual Design of a Single-Aisle Turboelectric Commercial Transport with Fuselage Boundary Layer Ingestion,* San Diego: AIAA, 54th Aerospace Sciences Meeting.